ATLAS BASED SEGMENTATION OF WHITE MATTER FIBER BUNDLES IN DTMRI USING FRACTIONAL ANISOTROPY AND PRINCIPAL EIGEN VECTORS

Esmaeil Davoodi-Bojd[1], Hamid Soltanian-Zadeh[1,2]

[1] Control and Intelligent Processing Center of Excellence, School of Electrical and Computer Engineering, University of Tehran, Tehran 14395-515, Iran
es.davoodi@ece.ut.ac.ir, hszadeh@ut.ac.ir

[2] Image Analysis Laboratory, Radiology Department, Henry Ford Hospital, Detroit, MI 48202, USA
hamids@rad.hfh.edu

ABSTRACT

In this work, we develop an atlas based method for automatic segmentation of white matter fiber bundles. To this end, we propose a new method for registration of diffusion tensor (DT) images using DTI information which is also used in the fiber tracking process, and we also propose a strategy for segmenting the fiber bundles using the new registration method and a probabilistic white matter atlas. We apply the registration method to 13 real DTI data sets and evaluate the results by comparing the level of alignment of all fibers. Then, we use the proposed strategy to segment 10 major fiber bundles in one of the subjects. One of the advantages of such a method is the robustness of the results thanks to using prior knowledge. The segmented results can be used for comparing and evaluating other fiber bundle segmentation methods.

Index Terms— DTMRI, Atlas based segmentation, White matter fiber bundles, Image registration

1. INTRODUCTION

Diffusion Tensor Magnetic Resonance Imaging (DTMRI) is a noninvasive tool for determining white matter connectivity in the brain. DTMRI adds to conventional MRI the capability of measuring the random motion of water molecules, referred to as diffusion [1]. The most important distinctive characteristic of DTMR images is that they have directional information of microtubule living structures. This can help us to determine white matter fiber bundle tracts, which can be helpful in diagnosing white matter diseases. Many methods for segmentation of fiber bundles have been proposed. Generally, the results of these methods are not similar due to using different strategies in each step of the segmentation process. On the other hand, atlas based image segmentation is a powerful method which benefits from prior knowledge, so it gives more robust and reliable results. However, this method has been rarely applied to segmentation of fiber bundles because of limitations of working with DTMR images. In this work, by proposing a new method for registration of DT images, we introduce an atlas based fiber bundle segmentation strategy.

Atlas based image segmentation consists of two main parts: a segmented and labeled image, called "atlas", and an image registration algorithm, which is used to align the atlas image to the subject image. The quality and performance of both of these parts determine the quality of the results. In [2] a good quality fiber tract atlas has been constructed which can be used in automatic segmentation. In this work, we use such an atlas.

Image registration is a critical step in atlas based imaged segmentation methods. However, applying conventional image registration methods to the DTMR images without considering orientation information of these images does not yield acceptable results. Thus, it has been proposed to use tensor reorientation methods when applying spatial transformation to the DTMR images [3], [4].

General registration using the whole tensor images generates better results [5]. However, for specific applications, certain parameters of the DTMR images can be more helpful in enhancing the results and reducing computational complexity. As the purpose of this study is to segment fiber bundles using registration, and in addition, most of fiber tracking algorithms use Fractional Anisotropy (FA) and Principal Eigen-Vector (PEV) maps, using these parameters are more appreciate. In [6], the DTMR images are registered based on FA images. However, until now, no one has used FA and PEV maps jointly for registration.

The aim of is this work is to develop an atlas based segmentation strategy for labeling white matter fiber bundles in two steps. First, we propose a new cost function for registering DT images based on aligning the fibers. We use this cost function on a piece-wise affine registration algorithm and also propose a method for combining the computed sub-transforms. Then, we use this registration method and a previously constructed probabilistic atlas of fiber bundles to label extracted fibers from DTMR images.

2. METHODS

2.1. DTI Registration

The aim of an image registration method is to find a transform between two images which aligns one of them to the other and maximizes the similarity between the transformed and target images. For DT images, the similarity function should consider the orientation of the tensors. In this paper, we use a combination of two features of DT images: FA map and the eigen-vectors corresponding to the maximum eigen-values of the DT images, which we call 'PEV map'. We chose these two features because many fiber tracking methods use them and also, the aim of this work is to propose a registration method for atlas based fiber bundle segmentation. The proposed cost function is an integral of two terms in each voxel: one for measuring the difference between FA values and the other for measuring the difference between the angles of PEV:

$$\phi(\underline{x}) = \int_{\Omega} [F_s(h(\underline{x})) - F_r(\underline{x})]^2 +$$

$$\omega.F_r(\underline{x}).[1 - E_s'(h(\underline{x})).Q.E_r(\underline{x})]^2 \, d\underline{x} \quad (1)$$

where F and E are the FA and PEV maps respectively, corresponding to the subject image, represented by 's', and the reference image, represented by 'r'. $h(.)$ represents the transform function of the spatial points $\underline{x}$, and Q is the 3×3 rotation matrix computed from the transform $h(.)$ for reorienting the Eigen-vectors, and finally, Ω is the region where the function is computed. Note that we call the moving image as 'reference image' and the target image as 'subject image'. The second part of this integral measures the angle differences over all voxels. Therefore, voxels with a low FA value and a high angle difference may cause the integral to compute a wrong measure. This can be compensated using the FA value of each voxel, $F_r(x)$. On the other hand, the two terms of this integral compute the differences by two different methods. So, their values may not be in a same range. Therefore, they must be weighted by a proper weight, ω. This cost function can be minimized using gradient descent methods because its derivative terms can be computed analytically.

2.1.1. Piecewise Affine Registration

In this work, we assume that the transform $h(.)$ is linear and can be expressed by an affine transform. An affine transform, $A_p(.)$, can be expressed by 12 parameters: 3 parameters for rotation ($\underline{q}$), 6 for deformation ($\underline{s}$), and 3 for translation ($\underline{t}$). Transformed point of $\underline{x}$ is:

$$h(\underline{x}) = (Q.S).\underline{x} + T = A_{\underline{p}}(\underline{x}) \quad (2)$$

where Q is the 3×3 rotation matrix with 3 independent parameters, S is the 3×3 deformation matrix with 6

independent parameters, T is the 3×1 translation vector, and finally, $\underline{p}$ is the whole unknown parameter vector $[\underline{q}, \underline{s}, \underline{t}]$.

In the piecewise affine registration, the images are divided into $n_x \times n_y \times n_z$ equal size sub-images and for each corresponding pair of sub-images (Ω^s_{ijk} and Ω^r_{ijk}, $i=1,\ldots, nx$, $j=1,\ldots, n_y$, $k=1,\ldots, n_z$) the cost function in (1) is minimized to find an affine transform parameters $\underline{p}_{ijk}$ for that region. In this work, we use a Conjugate Gradient (CG) algorithm to minimize (1). We also used an Evolutionary Algorithm (EA) to find the general region of the optimal parameters before applying the CG algorithm.

2.1.2. Estimating Transform Function

The remaining problem is: how to combine the resulting sub-transforms to build the final transformed image. This problem arises mainly in the border voxels of the sub-images. Reference [4] solves this problem by finding new sub-transforms for those voxels using interpolation between neighboring sub-transforms. However, this solution only considers limited number of neighbors to estimate the transformed border voxels. In [7], a method for estimating the transform function using a linear combination of Radial Basis Functions of some control points has been proposed:

$$\underline{y} = f(\underline{x}) = \sum_{i=1}^{N} \underline{a}_i.\exp\left\{-\left\|\underline{x} - \underline{x}_i\right\|^2 / \sigma^2\right\} + \underline{b} \quad (3)$$

where $\underline{x}$ is the coordinate of a spatial point in the reference image and $\underline{y}$ is the estimated corresponding point in the subject image, and $\{\underline{x}_i, i=1,...,N\}$ are N control points in the reference image. The equations for computing coefficients $\underline{a}_i$ and $\underline{b}$ have been calculated in [7]. This method has been applied on the scalar images for example FA images, but for DT images some modifications are needed. Therefore, for transforming PEV images, we compute the reorienting rotation matrix using the following equations.

Suppose for each voxel, the nonlinear function in (3) can be approximated by an affine transform, i.e.,

$$\underline{y} = f(\underline{x}) \equiv F_{\underline{x}}.\underline{x} + T \quad (4)$$

where $F_{\underline{x}} = Q_{\underline{x}}.S_{\underline{x}}$ is a linear transformation matrix. Differentiating both sides of (4) with respect to $\underline{x}$ gives,

$$J_f(\underline{x}) = -\frac{2}{\sigma^2}\sum_{i=1}^{N} \underline{a}_i.(\underline{x} - \underline{x}_i).\exp\{-\left\|\underline{x} - \underline{x}_i\right\|^2 / \sigma^2\} \equiv F_{\underline{x}} \quad (5)$$

where $J_f(\underline{x})$ is the Jacobian matrix of function $f(.)$. The rotation matrix can be estimated by (6) [3], and finally, the transformed image $E_t(.)$ of the reference image $E_r(.)$ can be expressed by (7), which consists of two transforms: spatial transform and reorienting transform.

$$Q_{\underline{x}} = (F_{\underline{x}}.F_{\underline{x}}^t)^{-0.5}.F_{\underline{x}} \quad (6)$$

$$E_t(f(\underline{x})) = Q_{\underline{x}}.E_r(\underline{x}).Q_{\underline{x}}^t \tag{7}$$

We consider a grid of points in the reference image, for example 8 corner points of a cube with half size in each dimension, centered on each sub-image and calculate the transformed points using the corresponding sub-transforms. Then, we employ these points as control points to estimate transformed image using the discussed method.

2.2. Registration Evaluation

The aim of the proposed registration algorithm is to be applied in an atlas based segmentation of fiber bundles. So, the strategy of evaluating the performance and capability of the method should consider the fibers. Thus, we compare the extracted fibers of the subject and transformed images.

In order to extract the fibers from the FA and PEV images, we use Dti-Studio software [8]. In this software, fibers are calculated based on the Fiber Assignment by Continuous Tracking (FACT) approach which is based on line propagation. This algorithm has 3 user defined thresholds: two for FA values and one for the angle. We chose both FA thresholds equal to 0.3 and the angle threshold equal to 70 degree.

Suppose the extracted fiber sets of the transformed and subject images are $F_t:\{l^t_1, l^t_2, ..., l^t_n\}$ and $F_s:\{l^s_1, l^s_2, ..., l^s_m\}$, respectively. n and m are the number of the fibers in the two sets. Each fiber l_i is a sequence of points. To compare the fiber sets, we define a measure as fallows:

$$d(F_t, F_s) = \frac{1}{m}\sum_{i=1}^{m} \min_j (H(l^s_i, l^t_j), j=1,...,n) \tag{8}$$

where $H(l^s_i, l^t_j)$ is the Euclidian based distance between fibers l^s_i and l^t_j which is defined as the average of pointwise minimum Euclidian distances between the fibers.

2.3. Atlas based Fiber Bundle Segmentation

To show the capability of the proposed method in automatic segmentation of fiber bundles, we used a probabilistic atlas of 10 major fiber bundles constructed at Johns Hopkins University [9]. We registered this atlas to a subject image and then transformed the label maps to it. Then, the extracted fibers from the subject image were labeled based on the transformed probabilistic labeled atlas. For this purpose, the probability of belonging each fiber f_i to each bundle B_j, i.e., $P(f_i|B_j)$ is computed using (9) and then, each fiber is assigned to the bundle with the highest probability (Bayesian Decision). In (9), we assumed that each fiber f_i goes through separate voxels $v_i(k)$, where $k=1,...,L$.

$$P(f_i | B_j) = \frac{1}{L}\sum_{k=1}^{L} P(v_i(k)|B_j) \tag{9}$$

3. RESULTS AND DISCUSSION

In this work, we used 13 DTMR image volumes acquired at Henry Ford Hospital, Detroit, MI using a 1.5T GE MRI (General Electric medical systems, Milwaunkee, WI, USA) from 13 healthy volunteers. The resolution of voxels in these data sets was different (0.9375×0.9375×3, 0.9375×0.9375×3.2, and 0.9375×0.9375× 5 mm). Therefore, we interpolated these images to get images with isotropic resolution of 1.875 ×1.875×1.875 mm and size of 128×128×80 voxels. Then, for each data set, tensor images and corresponding FA and PEV maps were computed using the method of [1].

To evaluate the proposed method for DT image registration, we select one of the data sets as the subject image and registered the other 12 images to it. Then, we extracted the fibers for each of the transformed image and calculated the dissimilarity between them and the fibers extracted from the subject using (8). In the registration cost function, (1), we selected ω=0.1. To investigate the effect of measuring the angles of PEV maps in the cost function (second term in (1)), we also chose ω=0 and repeated the test. In addition, we implemented the registration using the whole tensor [4] and then extracted the fibers for comparison. The results of applying this strategy are shown in Table 1. For better illustration, a typical result of applying the methods is shown in Fig. 1. It can be seen from this figure and Table 1 that using FA and PEV maps, registration results are enhanced. It seems strange that using less data the results are better. However, the fact is that the fibers are extracted only from the FA and PEV maps, which we used them in the registration. Thus, it is reasonable that the fibers are aligned more closely.

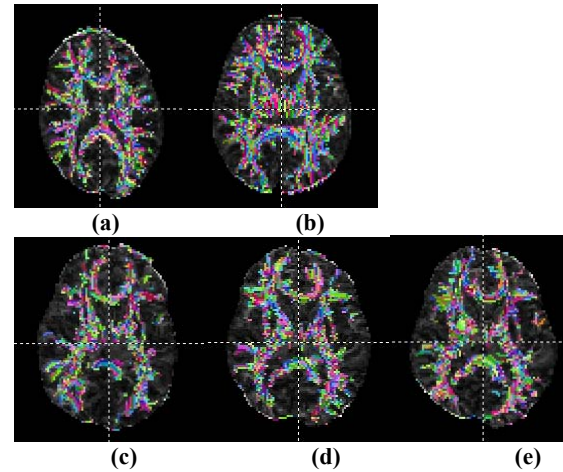**(a)** **(b)**

(c) **(d)** **(e)**

Fig. 1. Axial view of (a) reference image, (b) subject image, (c) and (d) transformed images computed from the registration using (c) the whole tensor and the proposed method with (d) ω=0 and (e) ω=0.1. The extracted fibers are shown with colored points. Note that the proposed method with ω=0.1 has aligned the fibers more accurately.
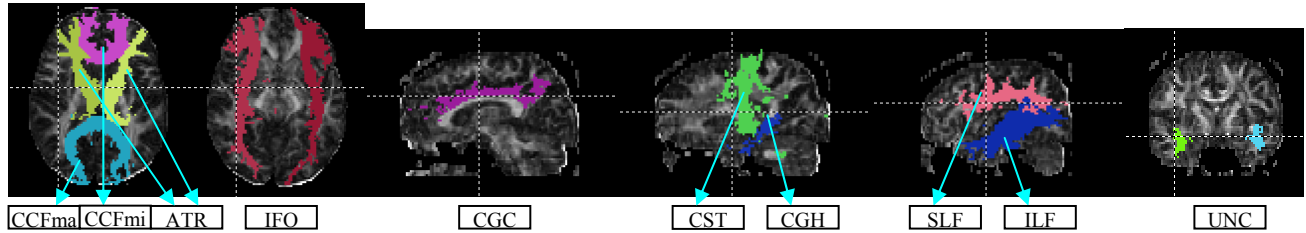
Fig. 2. Results of atlas based segmentation of 10 major fiber bundles for a typical subject. Corpus Callosum Forceps Major (CCFma), and Minor (CCFmi), Antenior Thalamic Radiation (ATR), Inferior Fronto-occipital Fasciculus (IFO), Cingulum Cingulate gyrus (CGC), and Hippocampus (CGH), Corticospinal Tract (CST), Superior Longitudinal Fasciculus (SLF), Inferior Longitudinal Fasciculus (ILF), and Uncinate Fasciculus (UNC).

The result of segmenting the fiber bundles for one of the data sets using the probabilistic white matter atlas is shown in Fig. 2. As this figure shows, the fibers are well clustered and segmented, and the results are reliable due to using prior knowledge of the atlas. Therefore, these results can be used for evaluating other fiber bundle segmentation methods such as fiber clustering methods where they suffer from weak strategies for evaluating the segmentation results.

4. CONCLUSION

In this paper, we conducted an atlas based method for automatic segmentation of white matter fiber bundles in two steps: 1) registration of DT images using the same information as that used in the fiber tracking process; and 2) segmentation of the fiber bundles using the proposed registration method and a probabilistic white matter atlas. We evaluated the registration method using 13 real DTI data sets by comparing the level of alignment of all fibers. The results show the superiority of the proposed method for aligning the fibers. Then, we used the strategy to segment 10

Table 1. Results of computing fiber dissimilarity (equation (10)) between the subject fibers and the fibers extracted from each reference image and the corresponding transformed images computed from the registration using the whole tensor and from the proposed method with ω=0 and ω=0.1.

Reference Image	Fiber Dissimilarity			
	Before Registration	Whole Tensor	ω=0	ω=0.1
#01	15.76	11.12	09.48	07.88
#02	08.83	07.89	07.45	07.09
#03	11.37	09.32	08.97	07.88
#04	08.61	07.53	07.14	07.03
#05	10.58	09.21	09.04	08.16
#06	32.71	19.18	16.12	14.43
#07	12.37	11.04	10.57	09.72
#08	17.29	14.77	12.24	10.98
#09	24.18	20.22	18.47	15.39
#10	12.32	12.15	11.91	11.30
#11	24.22	19.98	17.42	15.13
#12	18.77	13.21	10.97	09.25
Overall	**16.42**	**13.22**	**11.64**	**10.35**

major fiber bundles in one subject. One of the advantages of such a method is the robustness of the results thanks to using prior knowledge. One of the applications of this strategy is that the results can be used for comparing and evaluating other fiber bundle segmentation methods.

5. REFERENCES

[1] P.J. Besser, and D.K. Jones, "Diffusion-tensor MRI: theory, experimental design and data analysis –a technical review," *NMR in Biomedicine*, vol. 15, pp. 456-467, 2002.

[2] S. Wakana, H. Jiang, L.M. Nagae-Poetscher, P.C. van Zijl, and S. Mori, "A fiber-tract based atlas of human white matter anatomy," *Radiology*, vol. 230, pp. 77-87 , 2004.

[3] D.C. Alexander, C. Pierpaoli, P.J. Basser, and J.C. Gee, "Spatial transformations of diffusion tensor magnetic resonance images," *IEEE Trans. Med. Imag.*, vol. 20, no. 11, pp. 1131-1139, 2001.

[4] H. Zhang, P.A. Yushkevich, D.C. Alexander, and J.C. Gee, "Deformable registration of diffusion tensor MR images with explicit orientation optimization," *Med. Imag. Analysis*, vol. 10, pp. 764-785, 2006.

[5] H.J. Park, M. Kubicki, M.E. Shenton, A. Guimond, R.W. McCarley, S.E. Maier, R. Kikinis, F.A. Jolesz, and C.F. Westin, "Spatial normalization of diffusion tensor MRI using multiple channels," *Neuroimage*, vol. 20, no. 4, pp. 1995-2009, 2003.

[6] R. Larsen, M. Nielsen, and J. Sporring, "Improved correspondence for DTI population studies via unbiased atlas building," *MICCAI 2006, LNCS 4191*, pp. 260–267, 2006.

[7] D.Q. Peng, J. Liu, J.W. Tian, and S. Zheng, "Transformation model estimation of image registration via least square support vector machines," *Pattern Recognition Letters*, vol. 27, Issue 12, pp. 1397-1404, Sep. 2006.

[8] H. Jiang, P.C van Zijl, J. Kim, G.D. Pearlson, and S. Mori, "DtiStudio: resource program for diffusion tensor computation and fiber bundle tracking," *computer methods and programs in biomedicine*, vol. 8I, pp. 106–116, 2006.

[9] http://lbam.med.jhmi.edu/index.htm